Tellus (1995), 47A, 605–628
Printed in Belgium – all rights reserved

TELLUS
ISSN 0280–6495

Stages in the energetics of baroclinic systems

By ISIDORO ORLANSKI* and JOHN P. SHELDON, *Geophysical Fluid Dynamics Laboratory/NOAA, P.O. Box 308, Princeton University, Princeton, NJ 08542, USA*

(Manuscript received 5 September 1994; in final form 16 February 1995)

ABSTRACT

The results from several idealized and case studies are drawn together to form a comprehensive picture of "downstream baroclinic evolution" using local energetics. This new viewpoint offers a complementary alternative to the more conventional descriptions of cyclone development. These additional insights are made possible largely because the local energetics approach permits one to define an energy flux vector which accurately describes the direction of energy dispersion and quantifies the role of neighboring systems in local development. In this view, the development of a system's energetics is divided into three stages. In *Stage 1*, a pre-existing disturbance well upstream of an incipient trough loses energy via ageostrophic geopotential fluxes directed downstream through the intervening ridge, generating a new energy center there. In *Stage 2*, this new energy center grows vigorously, at first due to the convergence of these fluxes, and later by baroclinic conversion as well. As the center matures, it begins to export energy via geopotential fluxes to the eastern side of the trough, initiating yet another energy center. In *Stage 3*, this new energy center continues to grow while that on the western side of the trough decays due to a dwinding supply of energy via fluxes from the older upstream system and also as a consequence of its own export of energy downstream. As the eastern energy center matures, it exports energy further downstream, and the sequence begins anew. The USA "Blizzard of '93" is used as a new case study to test the limits to which this conceptual sequence might apply, as well as to augment the current limited set of case studies. It is shown that, despite the extraordinary magnitude of the event, the evolution of the trough associated with the Blizzard fits the conceptual picture of downstream baroclinic evolution quite well, with geopotential fluxes playing a critical rôle in three respects. First, fluxes from an old, decaying system in the Pacific were convergent over the west coast of North America, creating a kinetic energy center there and modifying the jet, resulting in a large extension of the overall kinetic energy center well into Mexico. Second, energy fluxes from this extension of the northwesterly flow were strongly convergent east of the trough, producing explosive growth of kinetic energy over the northwestern Gulf of Mexico, with baroclinic conversion following shortly thereafter. Lastly, the kinetic energy generated by the vigorous baroclinic conversion in the cold advection on the west side of the trough was very effectively transferred to the energy center on the east side of the trough via geopotential fluxes.

1. Introduction

Over the past 50 years, a large body of literature has been compiled regarding the evolution of extratropical cyclones, and today a great deal is known about baroclinic growth and barotropic decay. The early work by Sutcliffe (1947) and Petterssen (1956) on cyclone self-development emphasized the manner in which an approaching upper level wave helps to organize the low-level circulation such that it, in turn, intensifies the cyclogenetical processes of vorticity and thermal advection, thereby creating a positive feedback mechanism. Petterssen and Smebye (1971) distinguished between disturbances developing from the bottom up without any predecessor disturbance aloft ("type A"), and disturbances being triggered when

* Corresponding author.

a well defined vorticity maxima aloft passes over a pre-existing low-level baroclinic zone ("type B"). Analyses of developing storms using an energetics approach (Robertson and Smith, 1983; Dare and Smith, 1984) have primarily concerned themselves with volume integrals over a broad domain encompassing a particular cyclone (or anti-cyclone) or synoptic wave, and as such provide only minimal information about the processes occurring at points within the region. Nevertheless, important insights were obtained regarding the roles of in-situ energy generation, barotropic conversion, kinetic energy flux convergence, and frictional dissipation in the life cycle of extra-tropical cyclones. It is perhaps the potential vorticity (PV) approach which has provided the most insight regarding the dynamics of baroclinic development (Hoskins et al., 1985). One of the many benefits of the PV approach for diagnosing development was to provide a clearer understanding of type B cyclogenesis. It showed that the interaction of advancing pre-existing upper level PV anomalies with low level baroclinicity can explain many rather common cyclogenetic processes, and therefore represented a generalization of this class of cyclogenesis. While idealized simulations might provide valuable quantitative insight into the development of the trough associated with the pre-existing anomaly, there has been little success so far, probably because of the difficulty in posing an initial value which adequately portrays the conceptual model. Each of the different points of view described above has managed, in its own way, to clarify some aspect of the problem of individual cyclone development, and all of them have contributed to a more comprehensive understanding of the most important mechanisms regulating their growth and decay. However, as Hoskins (1990) points out, none of them provides a single, unique framework with which to understand the cyclone life cycle.

A related concept in cyclone evolution which is well known to synopticians is downstream development. The early work of Namias and Clapp (1944) and Hovmöller (1949) suggested that upper level trough development was correlated with the pre-existence of upstream systems. Renewed interest was shown in downstream development by Joung and Hitchman (1982), who analyzed Asian cold air outbreaks, and especially by the theoretical work by Simmons and Hoskins (1979) who demonstrated, using idealized simulations of the evolution of an initial localized perturbation on a simple basic state, that downstream development was possible in baroclinically unstable waves. However, it was difficult, both from the results of the idealized numerical simulations as well as from the existing documentation of real case studies, to distinguish the importance of this mechanism from other local sources of development.

Recent studies using a local energetics approach have been able to confirm, from both observational data and numerical simulations, the importance of downstream development in the life cycle of extratropical cyclones. Analysis of the development of cyclones in the eastern Pacific (Orlanski and Katzfey, 1991, hereafter O & K; Orlanski and Sheldon, 1993, hereafter O & S) suggested that the development of baroclinic eddies is as much a product of energy dispersed from decaying systems upstream as it is of classical baroclinic conversion. This limited set of individual case studies was bolstered by the findings of Chang (1993), who analyzed 8 years of winter data and found unequivocal evidence of downstream development along a considerable portion of the Pacific storm track.

The collective insight gained from the various studies described above now affords an opportunity to assemble a comprehensive picture for the development cycle of both individual kinetic energy centers and the entire ridge/trough system from an energetics standpoint. A brief review of the classical development theories is presented in Section 2, which also discusses the treatment of local energetics, the equations, the role of the ageostrophic geopotential flux structure in upstream and downstream development, and the eddy ageostrophic flow associated with a typical upper level trough. A comprehensive description of the energetics of an evolving downstream baroclinic system is presented in Section 3.

The important rôle played by downstream geopotential fluxes evidenced in the cases studied to date suggests that such fluxes may be a critical element in all developing baroclinic systems. To test the limit to which the energetics-based conceptual picture applies, and in an effort to determine whether baroclinic generation can be sufficiently intense as to make generation via flux convergence of only minor importance, a case study of the "Blizzard of '93" is presented in Section 4. The

explosive nature of this storm, the strong latent heat release, and its sheer size and intensity suggested tremendous baroclinic generation, making it an good candidate as a case which just might have developed without strong reliance on generation via flux convergence. The results indicate that, despite its extraordinary nature, the Blizzard actually fits quite well the overall pattern of downstream baroclinic evolution, with geopotential fluxes playing an important role not only as a significant source of kinetic energy during the early stages of development, but also in determining important features of the upper level trough associated with the storm prior to the development of the surface cyclone. Finally, a summary is given in Section 5.

2. Background

2.1. *Classical development theories*

A number of recent articles (Hoskins, 1990; Uccellini, 1990; Bosart, 1994) have provided extensive reviews of the various theories of extratropical cyclone development. The following provides a brief summary of the most outstanding contributions of each approach to our present understanding of cyclone and downstream development, and relates these more classical approaches involving quasigeostrophic theory and potential vorticity to a newer approach emphasizing local energetics.

The early work of Sutcliffe (1947) and Petterssen (1956) laid much of the groundwork on which synopticians and forecasters have relied for decades in diagnosing the structure of developing troughs. This work, which was based on the quasigeostrophic vorticity and omega equations and simple parameterizations of diabatic effects, provided a quantitative tool for describing the general characteristics of developing cyclonic systems. Their basic assumption was that the development of vorticity at low-levels implies upward motion above the area of development, as required by the vorticity equation. The omega equation was then used to diagnose the vertical motions which were required to maintain thermal wind balance. The omega equation can be derived by using the quasi-geostrophic vorticity (ζ_g) and the potential temperature equations and, following Hoskins (1990), can be expressed as:

$$f_0^2 \frac{\partial}{\partial z}\left(\frac{1}{\rho}\frac{\partial}{\partial z}\rho w\right) + N^2 \nabla^2 w = s_g + s', \tag{2.1}$$

where w is the vertical velocity, ρ is the density, f_0 is the Coriolis parameter at a reference latitude, N^2 is the Brunt-Vaisalla frequency, and s' is a source term involving β, friction, and diabatic heating. The term s_g is a source term involving only geostrophic quantities, which Sutcliffe approximated as

$$s_g \approx 2\left| f\frac{\partial v_g}{\partial z}\right| \frac{\partial \zeta_g}{\partial l}, \tag{2.2}$$

where l a coordinate oriented along the thermal wind $\partial v_g/\partial z$ and v_g is the geostrophic wind. For completeness, it should be noted that a more exact form for s_g was defined by Hoskins et al. (1978) which includes terms due to both thermal advection and vorticity advection, and was expressed as the divergence of a "Q vector". However, the Sutcliffe approximation, which is limited to the vorticity advection term, is simpler and adequate for discussion here. The left-hand side of (2.1) can be thought of as a kind of 3-dimensional Laplacian operating on w. With appropriate boundary conditions (such as $w = 0$ at the ground and at a certain height, H), this implies that the sign of w will be opposite that of s_g. Now, since s_g is negative downstream (along the thermal wind) of a vorticity maximum (typically found in the base of a trough), this implies upward motion and low level convergence there, which is favorable for the production of low level cyclonic vorticity (as well as upper level anticyclonic vorticity). The converse is true upstream of the vorticity maximum, with $s_g > 0$ implying downward motion, and thus anticyclonic tendencies near the surface and cyclonic tendencies aloft. The net effect is a tilting of the system as a whole, characteristic of a developing baroclinic wave.

Simmons and Hoskins (1979) used a similar argument to describe the mechanisms involved in downstream and upstream development for an initial-value problem in an Eady model. Through simple scaling arguments they showed that stretching is the dominant development mechanism for disturbances with scales on the order of the Rossby radius of deformation, with an initial cyclonic disturbance producing rising motion downstream and sinking motion upstream. The upward motion

induces convergence and cyclonic vorticity tendencies near the lower boundary ahead of the initial center, and divergence and negative tendencies near the upper boundary. The converse occurs upstream of the initial center, with cyclonic tendencies in the upper levels and negative vorticity tendencies at lower levels, with the net effect being a westward tilt of the vorticity. In time, the new anticyclonic centers downstream at the upper levels and upstream at lower levels will, themselves, produce tendencies with the opposite sign further downstream and upstream. This process continues in each direction away from the initial disturbance, producing new centers with vorticity of alternating sign, albeit with reduced intensity. Note that while the foregoing discussion was made in the context of a uniform baroclinic environment, it is easy to imagine that if a newly generated low-level disturbance was to form in an area of enhanced baroclinicity, the intensity of the development could be greatly enhanced because of both the reduced stability (see 2.2) and the stronger thermal wind (see 2.3). This case can be viewed as a simple model for type B cyclogenesis as proposed by Petterssen and Smebye (1971). The general phenomenon of downstream (and upstream) development will be discussed further from the point of view of local energetics in later sections.

A similar, but more general, conceptual picture of cyclone development can be obtained using potential vorticity arguments. The conservation properties and the invertability qualities of PV analysis have proven to represent a superb technique for investigating the dynamics of atmospheric systems. For a quasi-geostrophic system, knowledge of the internal distribution of PV and the surface potential temperature are sufficient to fully determine the system. In an enlightening review paper, Hoskins et al. (1985) described the use of PV analysis in meteorology and presented a clear description of extratropical cyclone development from a PV point of view. A simple picture is presented of the interaction of a pre-existing positive upper level PV anomaly with a surface baroclinic zone which also explains type-B cyclogenesis. In a manner similar to that posed by the previous arguments, the circulation at the ground which is induced by the upper level PV anomaly results in warm advection (due to the surface baroclinicity) slightly downstream of the PV maximum. This advection, in turn, enhances the cyclonic circulation which accentuates the advection of PV southward from high latitudes, increasing the magnitude of the existing PV anomaly and amplifying the entire development.

As valuable as all of these descriptions have been in fostering a better understanding of cyclone evolution, their primary usefulness has been in quantifying local sources and sinks (i.e., those within the radius of deformation). The effects of neighboring systems have been far more difficult to evaluate using these techniques. In the case of PV analysis, the selection of a characteristic isentropic surface is somewhat arbitrary and can be particularly difficult in highly perturbed cases. And while the flow field associated with a given anomaly can be determined using the invertability properties of PV, the results are subject to the choice of balance equation and boundary conditions (Davis and Emanuel, 1991).

Recently, diagnostics involving local energetics have been applied and shown to offer a valuable and complementary alternative to the above descriptions of the evolution of baroclinic systems. A series of both idealized and actual case studies (summarized below) has demonstrated that the growth of disturbances is a product of both baroclinic processes and the convergence of energy fluxes emanating from decaying systems. This viewpoint provides new insight into the energy transfer between individual centers which is key to downstream baroclinic development and can also help explain the origin of the pre-existing disturbance on which type B cyclogenesis is predicated. In addition, this approach has proven robust enough to provide an explanation of the mechanisms by which storm tracks are maintained far downstream from any strong baroclinic source. One important practical aspect of these diagnostics is that they permit the definition of an energy flux vector which describes, with sufficient accuracy, the direction of energy dispersion and quantifies the role of neighboring systems in local development. Another practical advantage of this technique is that the analysis can be reduced to 2 dimensions through vertical integration of the energetics components without any loss of relevance, so that one is not forced to choose a particular level or surface on which to work. It should be noted that the success with which these diagnostics have been applied is due largely to the radical improvements over the past several years

in the quality of operational analyses, which permit a more accurate retrieval of the ageostrophic fields.

The following sections provide a more complete description of how the diagnosis of local energetics can be used to obtain a better understanding of the processes of cyclone development. A comprehensive description of downstream baroclinic evolution is assembled based on the results of prior studies of local energetics, and a new case study is undertaken to test the robustness of this new approach.

2.2. *Local energetics approach*

As mentioned above, examination of the energy budget has proven to be quite useful in evaluating the origin and evolution of cyclones (O&K, O&S). By carefully separating the individual processes impacting system development, it is often possible to determine how and at what stage of development each process affects the system. Although regional energetics differ drastically from the classical Lorenz-averaged energetics (Lorenz, 1955) in the sense that balance in the conversion terms between mean and eddy components is not assured, ambiguities can be avoided provided one derives a self consistent set of equations for quadratic quantities such as the squared difference of the velocity amplitude or potential temperature. Interpretation of most of the source and sink terms are well established in the meteorological literature (Pedlosky, 1987; Peixoto and Oort, 1992) and are equally applicable to the regional derivation.

Chang and Orlanski (1993) demonstrated the value of this approach in their analysis of results from an idealized numerical model of systems developing along a storm track. The evolution of the volume mean eddy kinetic energy budget for two adjacent eddies along the storm track is shown in Fig. 1, where "eddy" is defined as a deviation from the time mean. The upper panel shows the evolution of the volume mean eddy kinetic energy in a frame following the motion of each eddy center (defined by a rectangular box centered on the maxima of eddy kinetic energy), with the appearance of the left eddy (i.e., upstream) preceding that of the right eddy by 3 days. The lower panel shows that the primary source of energy growth during the initial growth of the downstream eddy is the convergence of geopotential fluxes. Baroclinic generation does not become large until 2–3 days later, by which time the eddy is beginning to decay. The dominant sink during the decay stage is flux divergence. Further analysis led to the conclusion that downstream development of waves via this radiation of ageostrophic geopotential fluxes is the mechanism which enables the storm track to extend from a highly unstable region deep into regions of weak baroclinicity.

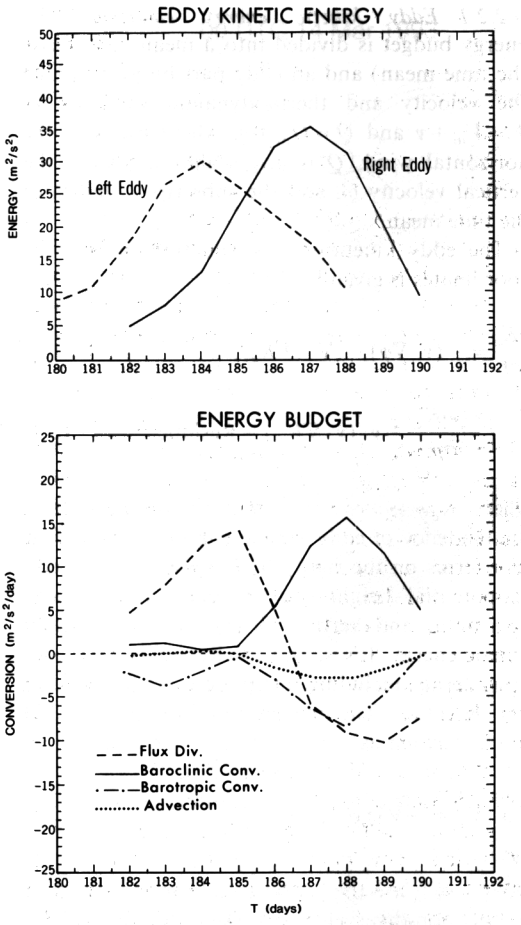

Fig. 1. Upper panel shows the evolution of volume mean eddy kinetic energy for two waves ("left" is upstream of "right") along a simulated storm track. Lower panel shows the evolution of the volume mean eddy kinetic energy budget for the "right" eddy, including the ageostrophic geopotential flux term, baroclinic conversion, barotropic conversion, and advection (adapted from Chang and Orlanski, 1993).

2.2.1. Eddy kinetic energy equation. The energy budget is divided into a mean part (here, the time mean) and an eddy part by partitioning the velocity and thermodynamic variables as $V = V_m + v$ and $Q = Q_m + q$, where the V is the horizontal wind, Q is any scalar, including the vertical velocity ω, and the subscript $_m$ indicates the time mean.

The eddy kinetic energy equation in pressure coordinates is given by:

$$\frac{\partial K_e}{\partial t} = -(v \cdot \nabla\phi) - (\nabla \cdot (VK_e))$$

$$-\frac{\partial(\omega K_e)}{\partial p} - v \cdot (v \cdot \nabla V_m) + \text{Residue}, \qquad (2.3)$$

where $K_e = \frac{1}{2}(u^2 + v^2)$. The term on the left is the tendency of eddy kinetic energy, and the first four terms on the right are the advection of eddy geopotential heights by the eddy velocity, the horizontal and vertical divergence of the eddy kinetic energy fluxes, and the Reynolds stress. All other terms, including dissipation, are included in the "Residue". The first term on the RHS of (2.3) can be written as:

$$-v \cdot \nabla\phi = -\nabla \cdot (v\phi)_a - \omega\alpha - \frac{\partial(\omega\phi)}{\partial p}, \qquad (2.4)$$

where $(v\phi)_a$ are the geopotential fluxes with most of the non-divergent part removed, defined by O&S as

$$(v\phi)_a = v\phi - k \times \nabla \frac{\phi^2}{2f(y)}. \qquad (2.5)$$

The first term on the RHS of (2.4) is the divergence of the ageostrophic geopotential fluxes and represents the dispersion of energy. The second term, $\omega\alpha$, represents (in an averaged sense) baroclinic conversion, i.e., the conversion of available eddy potential to kinetic energy. The third term is the vertical flux divergence which redistributes energy vertically via work done by pressure forces. Although this term can be large, its vertical integral over the depth of the atmosphere is generally very small, and it is the vertical integral (or average) of these quantities that is of relevance in the following discussions.

The vector $(v\phi)_a$ represents an important tool in diagnosing the growth and decay of disturbances, because it describes the direction of energy dispersion and quantifies the role of neighboring systems in local development. The following section illustrates how these fluxes can be used to gain some additional insight into the phenomena of upstream and downstream development.

2.3. Downstream versus upstream development

Studies of idealized flow (Simmons and Hoskins, 1979; Farrell, 1982; Hoskins, 1990; Orlanski and Chang, 1993) have shown that packets of unstable baroclinic waves can display downstream development behavior at the leading fringe of the packet at upper levels, and upstream development to the rear of the packet at low levels, due to energy fluxes. However, the distribution of these fluxes depends on the steering level of the baroclinic eddies. For waves that develop in an constant shear f-plane such as an Eady model, the steering level is in the middle of the channel and a strong symmetry is found in the fluxes: downstream in the upper levels and upstream in the lower levels. Surface friction and the westward movement due to β lowers the steering level and the eddies move with a mean speed more characteristic of the low level winds, producing an intensification of the downstream fluxes and a corresponding decrease in the upstream fluxes. Hoskins (1990) discussed the evolution at the fringe of the packet in terms of the dispersion of edge waves, supported by meridional gradients of potential temperature in the upper and lower lid. The geopotential flux field can be used to demonstrate that a similar explanation for the division of downstream and upstream fluxes can be obtained from a rather different point of view, presented below.

2.3.1. Ageostrophic geopotential flux structure. For *small amplitude quasigeostrophic waves*, the zonal ageostrophic flux responsible for the downstream/upstream development can be expressed as:

$$\frac{\phi}{f(y)} \frac{dv_g}{dt} = -u_a \phi. \qquad (2.6)$$

For almost neutral quasigeostrophic waves, assuming that d/dt can be approximated as $(U - C_{ph})(\partial/\partial x)$, (2.6) can be written as

$$(\bar{U} - C_{ph}) \frac{\phi}{f(y)} \frac{\partial(\phi_x)}{\partial x f(y)} = -u_a \phi, \qquad (2.7)$$

where the meridional geostrophic velocity has been replaced by $v_g = (\phi)_x/f(y)$, U is the mean flow at the level where the ageostrophic fluxes are evaluated, and C_{ph} is the phase velocity of the wave.

It is easy to show the horizontal average of (2.7) over a wavelength (assuming an approximately periodic wave) gives the approximate relation:

$$\overline{u_a\phi} = \tfrac{1}{2}(\bar{U} - C_{ph})\,\overline{v_g^2} \approx (\bar{U} - C_{ph})\,K_e. \qquad (2.8)$$

Note that this simple relation says that the sign of the fluxes, $u_a\phi$, is given by the sign of $(U - C_{ph})$.

Since the eddies are advected downstream with a speed, C_{ph}, characteristic of the low level winds (say, U(700 mb)), the ageostrophic fluxes will be the largest at upper levels, proportional to something like $U(300\text{ mb}) - U(700\text{ mb})$, and oriented in the downstream direction. If, however, U(700 mb) is larger than $U_{surface}$, the ageostrophic fluxes at low levels could be directed upstream from the wave center, as discussed in Orlanski and Chang (1993). Because both the eddy kinetic energy and $(U - C_{ph})$ are larger in the upper levels in cyclone waves, downstream fluxes at upper levels are typically much larger in magnitude than the upstream fluxes at lower levels. However, under special conditions (e.g., large meridional displacement of a system), upstream fluxes could be important in generating synoptic and mesoscale circulations (Thorncroft and Hoskins, 1990).

It is important to emphasize that (2.8) is applicable only in the context of small amplitude quasigeostrophic waves. It's inclusion here is simply for the purpose of illustrating the general relationship between the relative speed of the wind versus the wave, and the zonal component of the fluxes represented by $u_a\phi$.

2.3.2. Ageostrophic flow associated with a typical upper level trough. The reason for the predominantly downstream orientation of the geopotential fluxes at the upper levels (for a system that moves with mean speed smaller than the upper level flow) is illustrated in Fig. 2, which shows a conceptual sketch of a fully developed trough. The basic geopotential field at the upper levels is represented by two arbitrary contours at Φ_1 and Φ_2, and the wind flow through it is indicated by the solid curved vector. The ellipses oriented along the flow represent vertically averaged eddy kinetic energy centers, with the number and boldness of the lines

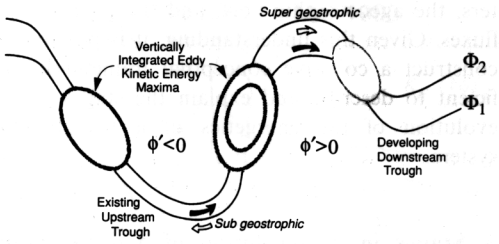

Fig. 2. Schematic illustration of the relationship between the components of a baroclinic wave. The upper level geopotential field is indicated by two contours labeled Φ_1 and Φ_2. The geopotential anomaly, Φ', relative to the time mean is positive/negative in the ridge/trough. Airflow relative to the wave is indicated by the heavy solid arrows and the ageostrophic wind is indicated by the open arrows. Centers of maximum vertically integrated eddy kinetic energy are shown as ellipses. An incipient disturbance is forming on the east side of the ridge at the center of the picture.

indicating the relative magnitude of the centers. As discussed by Lim and Wallace (1991), the upper level flow will be subgeostrophic ($u_a < 0$) in the trough and supergeostrophic ($u_a > 0$) in the ridge, as indicated by the open curved arrows. Now, assuming the mean circulation to be more zonal, the geopotential anomalies will be negative in the trough ($\phi' < 0$) and positive in the ridge ($\phi' > 0$). Thus, the correlation between the ageostrophic flow and the geopotential anomaly, ($u_a\phi'$), will be directed in the downstream direction at all points in the wave, as inferred from (2.7). Obviously, these fluxes will be largest in the middle of the trough and ridges, and will point from the exit region of the energy center on the west side of the upstream trough to the entrance region of the center on the eastern side of the trough, and from the exit region of that center to the entrance region of the incipient center on the eastern side of the ridge. Also evident from Fig. 2 is the fact that the ageostrophic flow at upper levels is divergent along the eastern side of a trough and convergent on the western side of a trough, implying descending motion on the western side of the trough and ascending motion on the eastern side, consistent with the concepts contained in the classical theories discussed earlier. The importance of these motions to the energetics will become more evident in the ensuing sections.

Thus, Fig. 2 is useful in helping to visualize the relationship between the trough, the energy cen-

ters, the ageostrophic flow, and the geopotential fluxes. Given this understanding, it is possible to construct a cohesive conceptual framework sufficient to describe and explain the stages in the evolution of the energetics of a trough/ridge system.

3. Stages in the evolution of a downstream baroclinic system

The following discussion will focus on the role of the various sources and sinks of eddy kinetic energy (see eq. (2.3)) in the evolution of a single trough. This evolution will be divided into three stages, as illustrated in Fig. 3. As in Fig. 2, the two solid lines represent arbitrary upper level geopotential height contours and the ellipses are the maxima in the vertically averaged kinetic energy. The wide arrows represent the vertical average of the energy fluxes at various points in the system, both advected K_e (solid) and those taking the form of geopotential fluxes (open). The partial ellipses attached to the energy centers contain "+" or "−" symbols representing sources or sinks of eddy kinetic energy, respectively. These sources/sinks include baroclinic and barotropic conversion terms as well as dissipation by surface

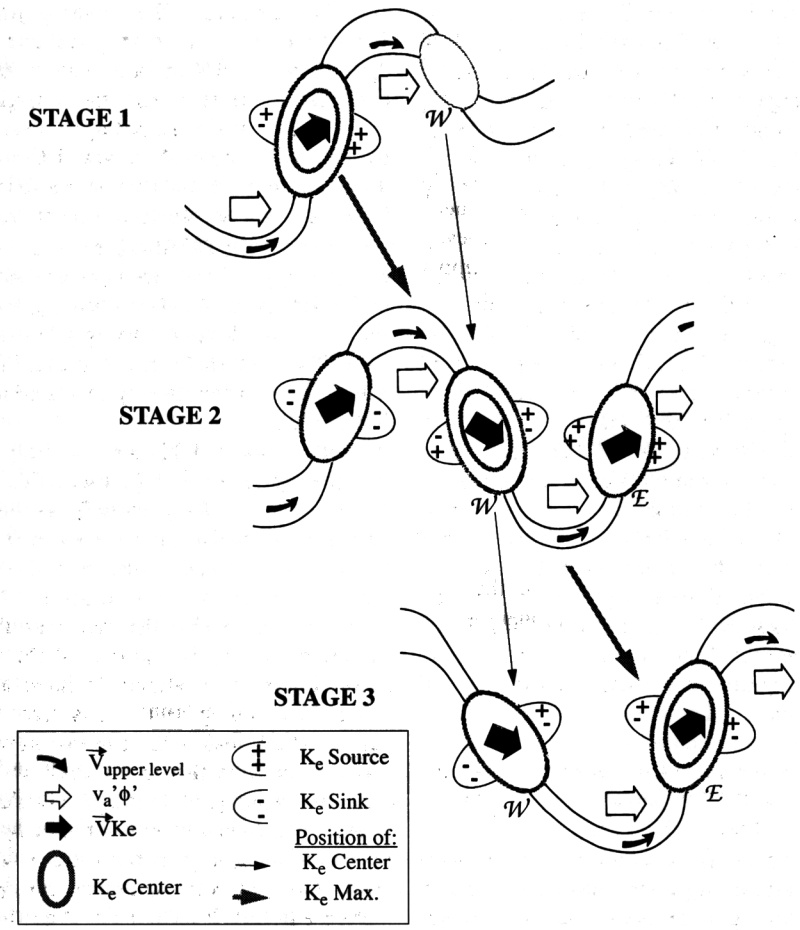

Fig. 3. The three stages in the evolution of a baroclinic wave. Symbols are as given in the figure. *Stage 1:* Upstream system decay and generation of energy center $\mathcal{W}$ west of new trough via geopotential fluxes. *Stage 2:* Energy fluxes emanate from a mature $\mathcal{W}$ and foster growth of energy center $\mathcal{E}$ east of trough. *Stage 3:* Dissipation of energy center $\mathcal{W}$, maturation of energy center $\mathcal{E}$.

friction. The dominance of one symbol over the other is indicative of net energy generation or dissipation within the particular energy center, although their positioning within the ellipses is arbitrary.

- *STAGE 1: Upstream system decay, generation of energy center $\mathcal{W}$ west of new trough*

To begin the sequence, a pre-existing trough with an associated kinetic energy center is assumed to be located upstream of an incipient trough. This older energy center is losing energy via geopotential fluxes through the ridge toward the entrance region of a new energy center, $\mathcal{W}$, which is beginning to grow on the western side of the developing trough. Note that, as discussed in the previous section, the fluxes are all oriented downstream, with flux divergence at the exit region of the old, pre-existing energy center and flux convergence at the entrance region of energy center $\mathcal{W}$. Kinetic energy generation ($-\mathbf{v}\cdot\nabla\phi$) in the vicinity of $\mathcal{W}$ at this time is almost entirely composed of flux convergence ($-\nabla\cdot(\mathbf{v}\phi)>0$) in the upper levels. This increase in kinetic energy is characterized by an increased geopotential height gradient at $\mathcal{W}$ supporting a stronger geostrophic wind and therefore higher kinetic energy. Note that the energy centers present at this time are actually the signature, in terms of energy, of the well known "jet streaks" (Uccellini and Johnson, 1979; Bluestein, 1993), and the formation of center $\mathcal{W}$ can be considered representative of the manner in which jet streaks are generated. Note also that although the centers of convergence and divergence associated with the conceptual picture of isolated jet streaks are not the same as those in the environment of a large trough (such as that shown in Fig. 2), the direction of the ageostrophic flow across the streak is, of course, the same.

- *STAGE 2: Energy fluxes from mature $\mathcal{W}$, growth of energy center $\mathcal{E}$ east of trough*

While energy center $\mathcal{W}$ is undergoing growth due to convergent energy fluxes, subsidence west of the trough is taking place due to the convergence of the ageostrophic circulation at upper levels. Because this sinking motion takes place in a cold anomaly (for a baroclinic system), this implies additional generation of kinetic energy via baroclinic conversion ($-\omega\alpha>0$). However, flux divergence at the exit region of $\mathcal{W}$ (due to westward ageostrophic circulation at the base of the trough, see Fig. 2) will constantly remove energy from that center and deposit it on the eastern side of the trough, contributing to the development of another new energy center, $\mathcal{E}$. The divergent upper level ageostrophic flow on the eastern side of the trough induces upward motion there. Since this is an area which is typically a warm anomaly, the general flow will be characterized by warm ascending motion, implying baroclinic generation, contributing additionally to the energy of center $\mathcal{E}$. However, it is important to note that this baroclinic conversion takes place well after the initial kinetic energy growth due to flux convergence. It is the flux convergence at upper levels which initially acts to intensify the new energy center (and the trough), thereby enhancing the warm ascending motion. This warm ascent slowly deepends to reach the lower levels where baroclinicity is typically more intense. This is precisely the sequence of events characterizing type-B cyclogenesis, but expressed in terms of eddy kinetic energy. The induced upward motion can be further intensified by latent heating and increased buoyancy, resulting in strong upper level divergence. This, in turn, leads to increased fluxes, some of which can export energy to yet another system downstream.

Another aspect of this general flow pattern is the flux of eddy kinetic energy itself, $\mathbf{V}K_e$ (filled bold arrows in Fig. 3). While these fluxes are large, they act mainly to redistribute energy from the rear to the front of the energy center and not between energy centers, as is the case for geopotential fluxes. To emphasize the fact that the effective advecting velocity is not that of the upper level wind, the vector is shown to have a somewhat larger zonal component. It is this zonal component which makes the system move eastward, and the speed of the center itself given by C_{ph}, the phase velocity. Note that the meridional component of the flux vector is not actually effective in advecting the energy center meridionally, because most of the meridional energy transport to the leading edge of the energy center via $\mathbf{V}K_e$ is, in fact, removed via geopotential flux divergence ($-\nabla\cdot(v\phi)>0$) to the system downstream. This process affects energy centers on both the eastern and western side of a trough, and explains why

energy maxima are not actually advected through the top of a ridge or the base of a trough. Instead, the energy centers will be seen to "jump" from one side of the ridge or trough to the other. This process takes place with a speed C_g (the group velocity) which, in this case, is larger than the phase velocity, C_{ph}. This distinction is illustrated in Fig. 3 by the long arrows connecting the first, second, and third pictures. The long, thin arrow indicates the position of a single energy center throughout its life cycle, its displacement defining C_{ph}. The long, heavier arrow follows the energy maximum, the displacement of which defines the group velocity. As discussed in Orlanski and Chang (1993), it is possible to generalize the group velocity in a large finite amplitude system from the linear concepts and can be shown to be the sum of two terms: the advected velocity (C_{ph}) and relative group velocity, C_{gr}, the latter defined as the geopotential fluxes divided by the total eddy energy. The total group velocity, $C_g = C_{ph} + C_{gr}$, for downstream development is, in this case, larger than the C_{ph} (since the geopotential fluxes are all positive) and close to the upper level wind velocity. A possible interpretation for this is that because the trough moves at a mean speed corresponding to the wind in the middle of the troposphere (which is slower than the upper level winds), the signal in the upper levels (where downstream development is important) is carried by the wind at approximately those levels (Simmons and Hoskins, 1979; Orlanski and Chang, 1993).

The relationship between severe weather and jet streaks is well documented in the literature, and have been observed in both the polar and subtropical jets (for a review, see Bluestein (1993)). While it is certainly possible that there exist different mechanisms for generating jet streaks, the type to which we are referring here are those associated with baroclinic systems, and these will behave as described above, consistent with energy dispersion from one energy center to the next one downstream. This "jumping" of energy centers is due to the action of geopotential fluxes. This is consistent with the observed behavior of jet streaks, which are commonly found in the northwesterly flow west of a trough but typically *reform* on the eastern side of a trough, as opposed to being being continuously *advected* through the trough (Newton and Palmen, 1963). While it may be possible in some highly distorted cases for a jet streak to be found at the base of the trough (Shapiro, 1982), an analysis of the energetics shows that, for the more typical case, it is the ageostrophic circulation which induces the secondary energy center (and the associated jet streak) by transferring energy from the leading edge of one jet streak to another center downstream.

- *STAGE 3: Dissipation of energy center $\mathcal{W}$, maturation of energy center $\mathcal{E}$*

Once the supply of energy via geopotential fluxes from the upstream system ceases, center $\mathcal{W}$ will begin to decay, primarily through the divergence of geopotential fluxes which are transferring energy downstream to center $\mathcal{E}$, which also continues to intensify through vigorous baroclinic conversion associated with ascending warm air. Baroclinic conversion within $\mathcal{W}$ may continue for some time, providing an indirect energy source for $\mathcal{E}$ by virtue of the fluxes exiting $\mathcal{W}$. Barotropic decay and surface friction may also contribute to the decay of $\mathcal{W}$. Eventually, $\mathcal{W}$ decays to the point where it is no longer supplying energy to $\mathcal{E}$ via fluxes, and baroclinic conversion becomes the sole source of energy for $\mathcal{E}$. Meanwhile, divergent fluxes from the downstream end of $\mathcal{E}$, together with barotropic conversion and frictional effects, are all acting as sinks of energy for $\mathcal{E}$. Depending on the intensity of the baroclinic generation relative to these sink terms, the kinetic energy center may keep growing for some time, but will eventually resemble the "upstream" center depicted in the Stage 1 picture.

This conceptual picture, in which an upper level disturbance is organized well before any baroclinic conversion is present, embodies the general concept of type B cyclogenesis. If, as it seems, such a sequence is part of the development of baroclinic systems in general, pure baroclinic development would likely be the exception, perhaps limited to such areas as the entrance of the Pacific storm track, where baroclinicity is large and fluxes from upstream might be negligible (for lack of upstream systems themselves). Of course, the strength of the various sources and sinks in any system defines a broad spectrum of possible developments. For conditions of weak baroclinicity, development will be limited to upper levels and the disturbances will more closely resemble the wave packets discussed earlier. In the case of moderate baroclinicity and fluxes, deep structures can be generated. If the

baroclinicity is very strong, explosive developments can ensue. Such systems will likely owe much of their decay to "wave breaking" and strong surface friction, reducing the effectiveness with which energy is fluxed to a new system downstream. If this were not the case, one would observe well organized packets of energy moving around the globe at all times. While such long-lived packets have been observed in some parts of the globe (Lee and Held, 1993; Chang, 1993; Randel et al., 1987), such is not the case in general.

4. A case study: the Blizzard of '93

Although the number of cases examined to data is admittedly small (both real and idealized), the apparent pervasiveness of downstream energy fluxes suggests that it may be an important mechanism in virtually every cyclone. What is not yet clear is whether there exist cases which are so dominated by baroclinic conversion that geopotential flux convergence constitutes only a minor factor in the initiation of the system. It is also of interest whether, under extreme conditions, the geopotential fluxes would behave in the same way as they have been observed to date. With this in mind, the so-called "blizzard of '93" was chosen for study as a test case. The magnitude of this event certainly satisfies the requirements for testing under extreme conditions, and the tremendous amounts of latent heat release implied by the extraordinary precipitation amounts, and its development in an otherwise quiet region, point to this as a case where baroclinic conversion had a major, perhaps overwhelming, role in the development of the system.

The discussions in this section are based on the standard NMC analyses on a $2.5° \times 2.5°$ grid, which is available at 12-h intervals. In the following sections, the term "analysis" will refer to this data. These analyses were used not only to diagnose the synoptic features of the storm, but also proved quite adequate for calculating most of the terms of the energy budget. This was verified using numerical simulations which produced results entirely consistent with those based on analyses alone, thus providing confidence in the internal consistency of the analyses.

4.1. Synoptic description

4.1.1. Weather synopsis. Prior to 00 UTC 13 March, the only low pressure system evident from the 12-hourly NMC analyses was located over the central Gulf of Mexico, and the northern Gulf of Mexico was very quiet. (Higher resolution hand analyses do indicate a better defined low center over the western Gulf at this time, however.) The cyclone which was to become the Blizzard of '93 began explosively during the next 12 h and by 00 UTC 13 March was located along the Gulf coast of Texas and Louisiana. Detailed synoptic reports during the subsequent 12 h showed a compact system which moved along the Gulf coast and into eastern Georgia, spawning more than two dozen tornadoes in Florida and generating a 9 foot storm surge along the Florida coast. By 00 UTC 14 March, the storm had deepened significantly and was positioned over Chesapeake Bay. Fig. 4 depicts the sea level pressure distribution at this time and also indicates the track of the storm and its position at 12-h intervals. During the 24-h period from 00 UTC 13 to 00 UTC 14 March, the storm deepened by over 31 mb, easily qualifying as a "bomb" (Sanders and Gykum, 1980). As the storm moved up the east coast, numerous snowfall, pressure, and temperature records were set, wind gusts in excess of $30\ m\ s^{-1}$ (60 kts) were common, and every major airport on the east coast was closed at some time. While the Blizzard of '88 was probably more severe in the northeast, the area affected by the Blizzard of '93 was far larger, with snowfalls of up to 15 cm measured as far south as the Florida panhandle, and amounts of 60–120 cm in interior regions along the Appalachians from Georgia to New England (Lott, 1993).

4.1.2. Upper levels. The evolution of the upper level flow is summarized in Figs. 5 and 6, which show the analyzed 500 mb height field and the Ertel potential vorticity on the 325 K surface, respectively. A relatively small wave can be seen to move across the northern USA from 10–12 March, while a wave initially in the southern branch of the westerlies over the eastern Pacific moved into the desert southwest and northern Mexico. A separate wave in the northern branch strengthened and was positioned over the central western North America by 00 UTC 12 March. By 00 UTC 13 March, the southern wave penetrated well into the Gulf of Mexico and the northern wave reached the Gulf coast at around 265° E. The PV intrusion extended south into the western Gulf and became quite narrow, in large part due to the destruction

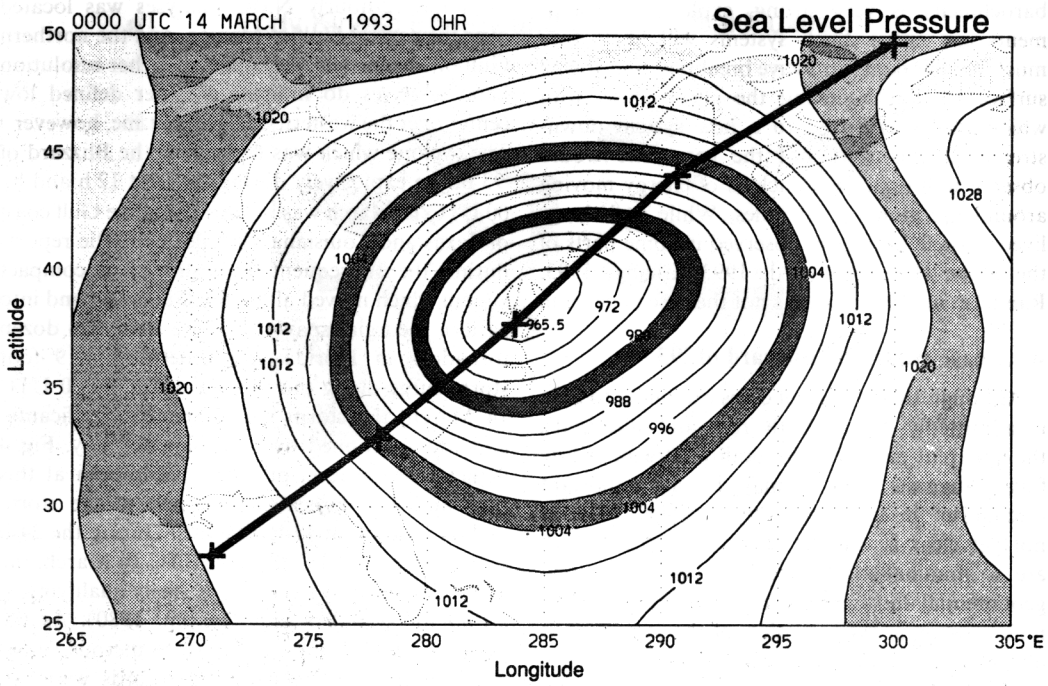

Fig. 4. Analyzed sea level pressure distribution at 0000 UTC 14 March (contour interval = 4 mb) and track of surface cyclone (crosses indicate position at 12-hourly analysis cycle).

of PV on the 325 K surface by deep latent heat release over the southeastern USA. After this time, the overall trough deepened dramatically over the eastern USA, with the PV pattern reflecting the strong circulation characteristic of the mature system.

4.2. *Energetics*

Fig. 7 shows the vertically averaged (50 mb to surface) eddy kinetic energy, K_e, together with the vertically averaged $(v\phi)_a$ fluxes, for a 12-h sequence from 12 UTC 11 March through 00 UTC 14 March. The same basic features found in the height and PV pattern can be identified as parts of the K_e field, but it is also possible to identify and track individual energy centers as distinct features in and of themselves. In addition, the $(v\phi)_a$ fluxes immediately suggest that energy flux between centers will be an important part of the life cycle for each energy center.

A fairly broad energy center over western North America at 12 UTC 11 March is seen to consist of two separate maxima. The flow at this time can be fairly characterized as Stage 1, with strong geopotential fluxes associated with a system farther out in the Pacific convergent in the area of the southernmost maximum. These fluxes continue for another 12–24 hours and the two separate maxima merge, with the previous southern maximum forming a long southward extension to the energy center as a whole. Note the correspondence between the kinetic energy and PV patterns (Fig. 6), with high values of PV lying just to the left (looking downstream) of areas of high K_e.

Through 12 UTC 12 March, the Gulf of Mexico region was extremely quiet. Fluxes into the region are beginning at this time, originating from the southern end of the primary energy center to the west. The energy center on the east side of the developing trough is beginning to show some intensification (although this is not the center which is to become the ultimate core of the Blizzard). At this point, the energy center on the western side of the trough moves southeast toward the Gulf of Mexico, but does not undergo any further net growth. In general, the pattern is beginning to resemble Stage 2.

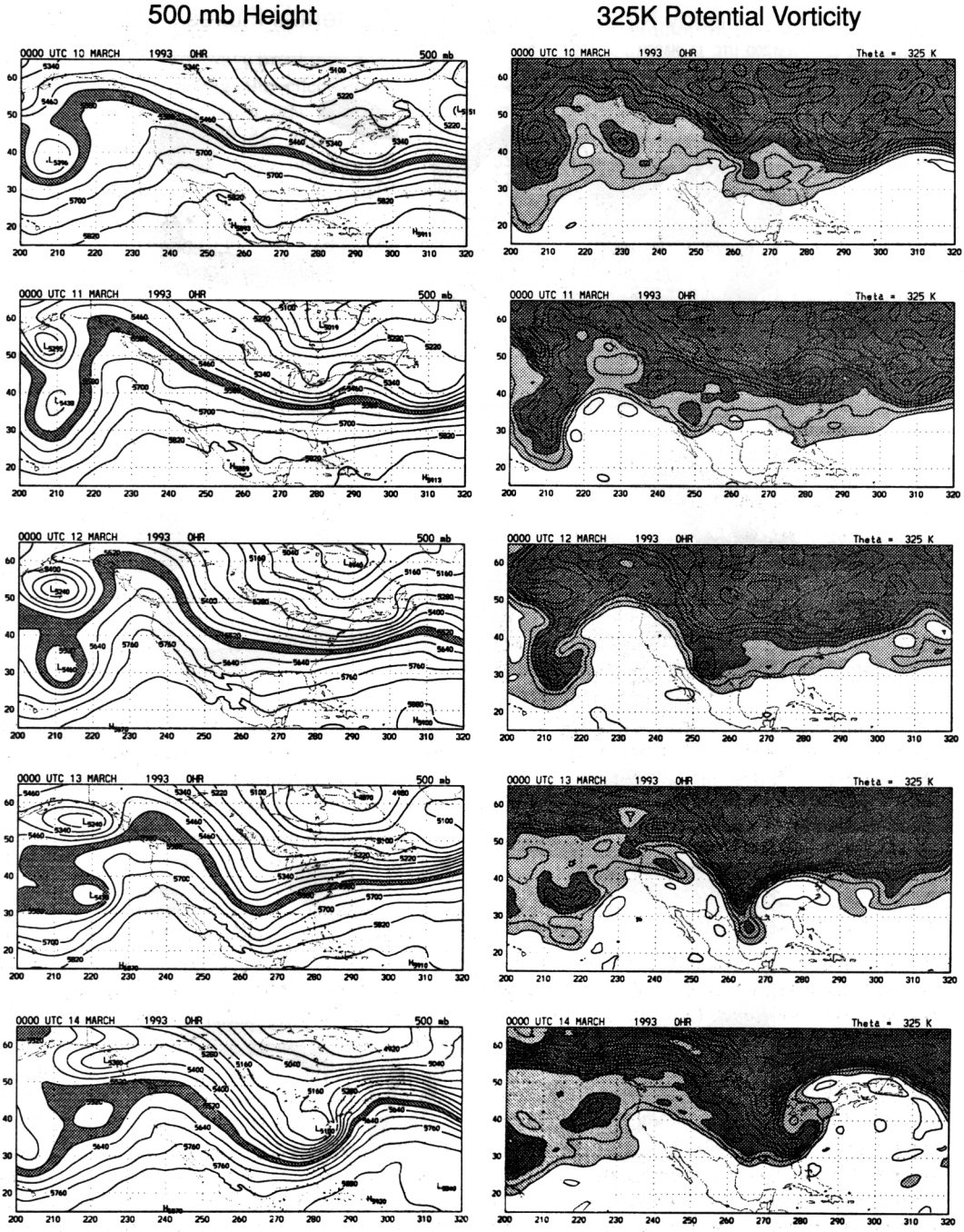

Fig. 5. 500 mb height field at 24 h intervals from 0000 UTC 10 March through 0000 UTC 14 March. The contour interval is 60 m, and heights between 5520 and 5580 m are shaded.

Fig. 6. Ertel potential vorticity on the 325 K surface at 24-h intervals from 0000 UTC 10 March through 0000 UTC 14 March. Light and dark shading indicate areas with PV in excess of 1 and 3 PV units, respectively.

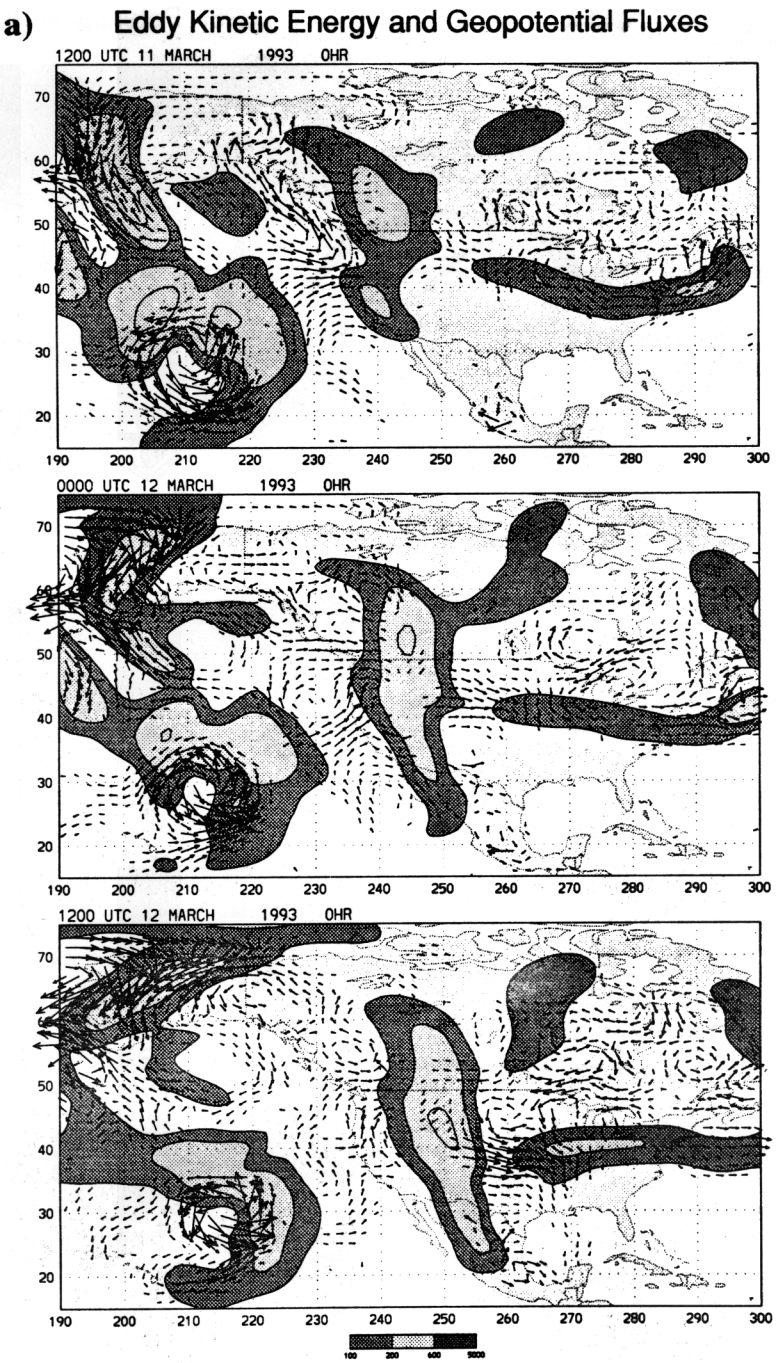

Fig. 7. Sequence, at 12-h intervals, of the vertically averaged (50 mb to surface) eddy kinetic energy, K_e, and divergent component of the geopotential fluxes. Contours are drawn at 100 $m^2 s^{-2}$, and at 200 $m^2 s^{-2}$ intervals starting at 200 $m^2 s^{-2}$. Medium, light, and dark shading indicates K_e greater than 100, 200, and 600 $m^2 s^{-2}$, respectively.

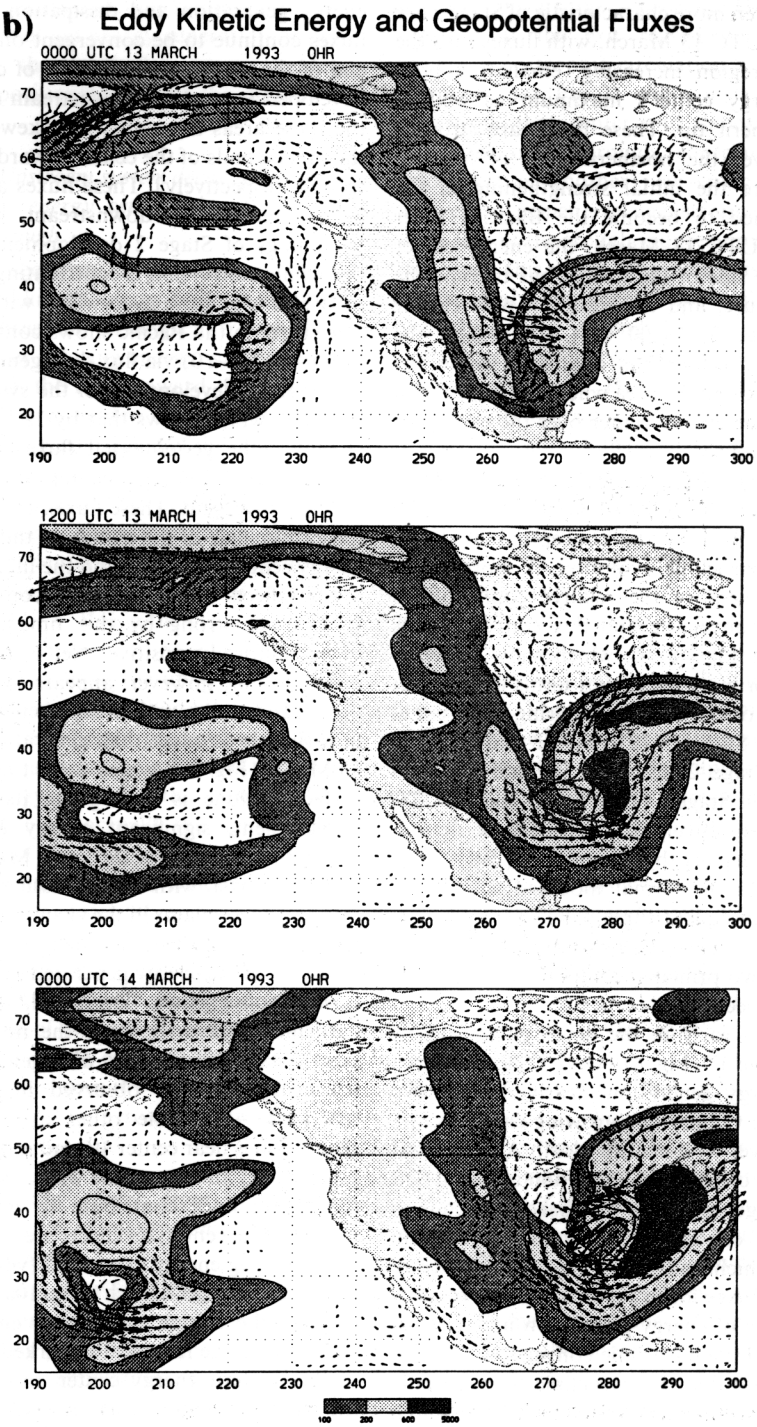
b) Eddy Kinetic Energy and Geopotential Fluxes
0000 UTC 13 MARCH 1993 0HR
1200 UTC 13 MARCH 1993 0HR
0000 UTC 14 MARCH 1993 0HR
70
60
50
40
30
20
190 200 210 220 230 240 250 260 270 280 290 300

Fig. 7 (cont'd).

Processes even more characteristic of Stage 2 are evident at 00 UTC 13 March, with fluxes into the Gulf coastal region increasing, emanating both from the energy center's maximum as well as from its southern tip. These fluxes are strongly convergent over the northern Gulf of Mexico, precisely where the initial strengthening of the cyclone destined to become the Blizzard takes place. By 12 UTC 13 March, the energy center on the eastern side of the trough has become the dominant feature, and the situation now closely resembles Stage 3. At 00 UTC 14 March, the original energy center has dissipated (note the strong fluxes exiting the area where the center used to be), while the energy center over the east coast grows tremendously.

Thus, it appears from Fig. 7, at least superficially, that even the Blizzard of '93 followed the sequence described by the conceptual model of downstream baroclinic evolution. A more quantitative assessment of the relative contributions of baroclinic conversion and flux convergence is obtained from Figs. 8–10, which show a breakdown of the primary energetics terms throughout the evolution of the trough, covering what could be considered Stage 1 (12 UTC 11 and 00 UTC 12 March), Stage 2 (12 UTC 12 and 00 UTC 13 March), and Stage 3 (12 UTC 13 and 00 UTC 14 March), respectively. In each of these figures, the top panel depicts the K_e and $(v\phi)_a$ fields as in Fig. 7, but with the format modified slightly for clarity. The subsequent three panels for each time show the primary energy generation term, $-\boldsymbol{v}\cdot\nabla\phi$, as well as its two principal components, $-\nabla\cdot(\boldsymbol{v}\phi)$ and $-\omega\alpha$, respectively.

The patterns early in the development closely resemble "Stage 1" (Fig. 8). At 12 UTC 11 March (Fig. 8a), energy generation clearly exceeds dissipation in the vicinity of a growing energy center (labeled $\mathcal{W}$) over west-central North America and along the west coast. This generation is dominated by flux convergence effects, with baroclinic conversion a minor contributor. A mature system in the Pacific, which constitutes the main source of geopotential fluxes for $\mathcal{W}$, is seen to have roughly equal amounts of energy generation and dissipation, but very little baroclinic conversion. (In fact, it would appear that the baroclinic term actually constitutes an energy sink.) By 00 UTC 12 March (Fig. 8b), energy center $\mathcal{W}$ has strengthened considerably, and now possesses regions of both energy generation and dissipation. Geopotential fluxes continue to be convergent on the upstream end of the center, and a region of divergence has developed toward the downstream end (although the these areas are somewhat skewed away from the precise ends of the center toward the ridge and trough, respectively). These fluxes are convergent in an area 10–15° downstream, suggesting the beginnings of Stage 2 development. Meanwhile, baroclinic conversion is contributing to the energy of $\mathcal{W}$ and is positive everywhere within the center. The storm in the Pacific shows continued dissipation ($-\boldsymbol{v}\cdot\nabla\phi<0$) via flux divergence.

"Stage 2" development of the system is evident in Fig. 9, which shows that by 12 UTC 12 March (Fig. 9a), the geopotential fluxes on the downstream side of energy center $\mathcal{W}$ are becoming strongly divergent. These fluxes are convergent on the eastern side of the trough in the vicinity of the energy center labeled $\mathcal{E}$, and the increase in energy levels reflects this. Baroclinic conversion within $\mathcal{W}$ is quite strong by this time and continues to be uniformly positive. Net energy generation ($-\boldsymbol{v}\cdot\nabla\phi<0$), however, appears to have changed sign at this point, with areas of energy dissipation now slightly stronger than generation. At 00 UTC 13 March (Fig. 9b), which is the time at which the surface cyclone is undergoing its strong initial development, significant energy generation via $-\boldsymbol{v}\cdot\nabla\phi$ is evident over the lower Mississippi valley and Gulf coast, with energy dissipation dominant over the lower plains in the vicinity of the center $\mathcal{W}$. Examination of the component terms reveals that nearly all of the energy generated in center $\mathcal{E}$ is due to flux convergence. The small, intense area of baroclinic generation over the northern Gulf is largely canceled by flux divergence, a situation which is frequently observed in areas of concentrated $-\omega\alpha$. The other area of baroclinic generation is near center $\mathcal{W}$, and is a product of the sinking cold air west of the wave. While baroclinic conversion does contribute to maintaining the energy of the center, its effects are more than offset by the strong energy export via $(v\phi)_a$.

By 12 UTC 13 March (Fig. 10a), the development of the trough has clearly entered Stage 3. While this stage is typically marked by dissipation of the western energy center and maturation of the eastern center, this case deviates slightly from the pure conceptual picture in that energy center $\mathcal{E}$ is continuing its unusually robust growth

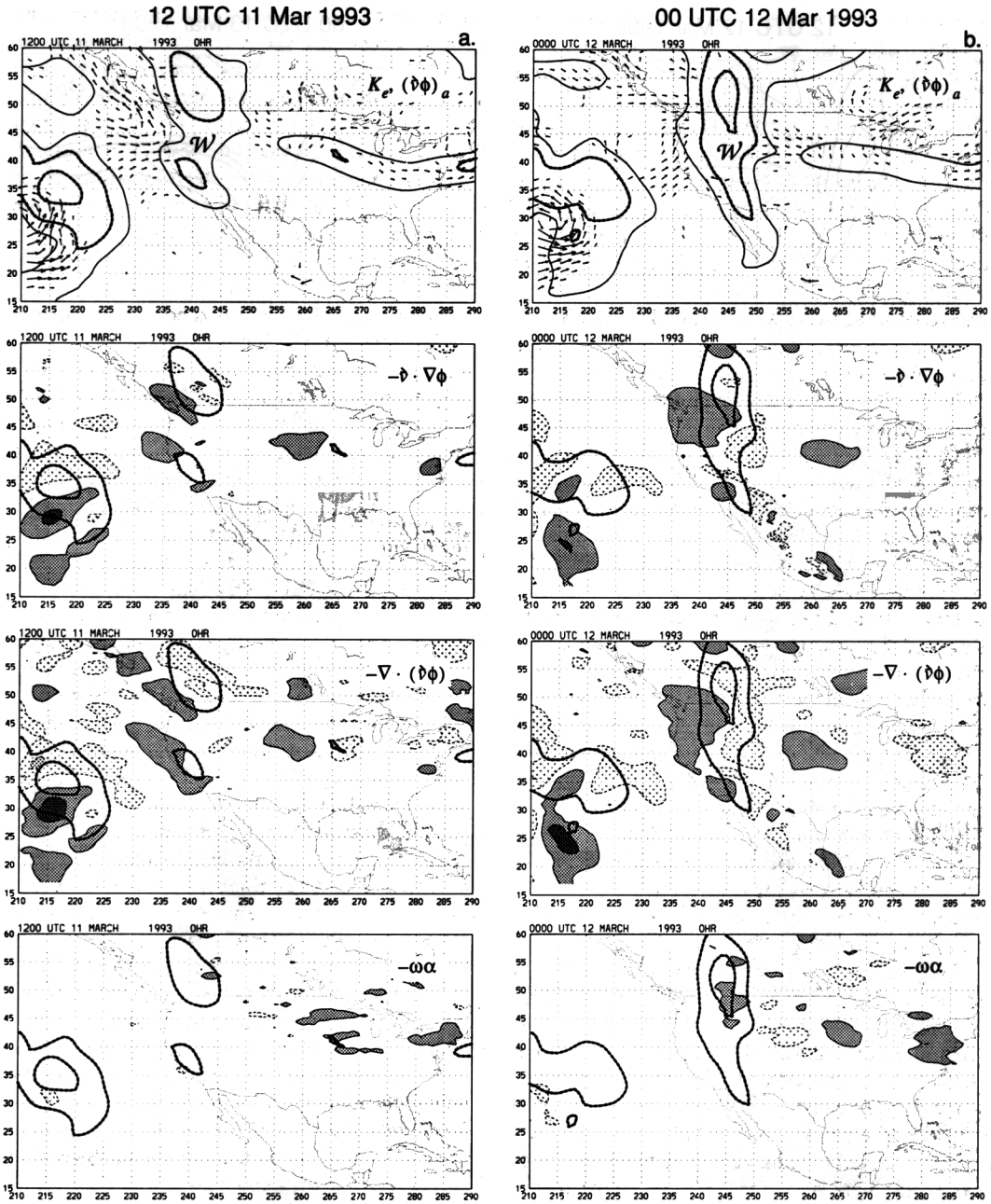

Fig. 8. Energetics at (a) 1200 UTC 11 March and (b) 0000 UTC 12 March. Top panel: vertically averaged (50 mb to surface) eddy kinetic energy, K_e, and divergent component of the geopotential fluxes. Contours are drawn at 100, 200, and 350 $m^2 s^{-2}$. Second panel: vertically averaged eddy kinetic energy and $-\nu\cdot\nabla\phi$. Third panel: vertically averaged eddy kinetic energy and geopotential flux convergence, $-\nabla\cdot(\nu\phi)$. Bottom panel: vertically averaged eddy kinetic energy and baroclinic generation, $-\omega\alpha$. For the bottom three panels: K_e contours at 200 and 350 $m^2 s^{-2}$; light and dark shading indicate energy generation of 5×10^{-3} and 15×10^{-3} $m^2 s^{-3}$, respectively, and light and dark stippling indicate energy dissipation of -5×10^{-3} and -15×10^{-3} $m^2 s^{-3}$, respectively.

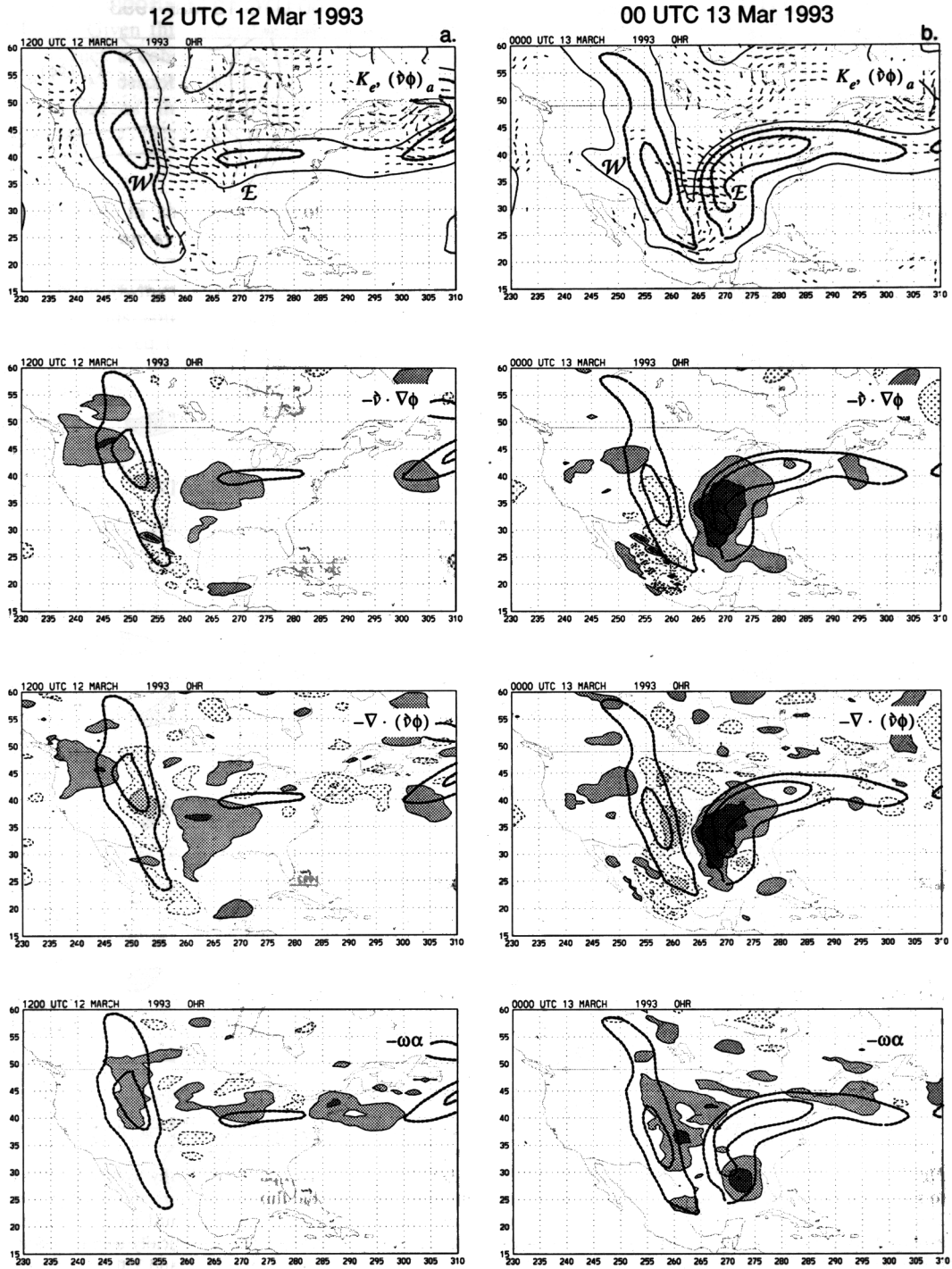

Fig. 9. Same as Fig. 7, but for (a) 1200 UTC 12 March and (b) 0000 UTC 13 March.

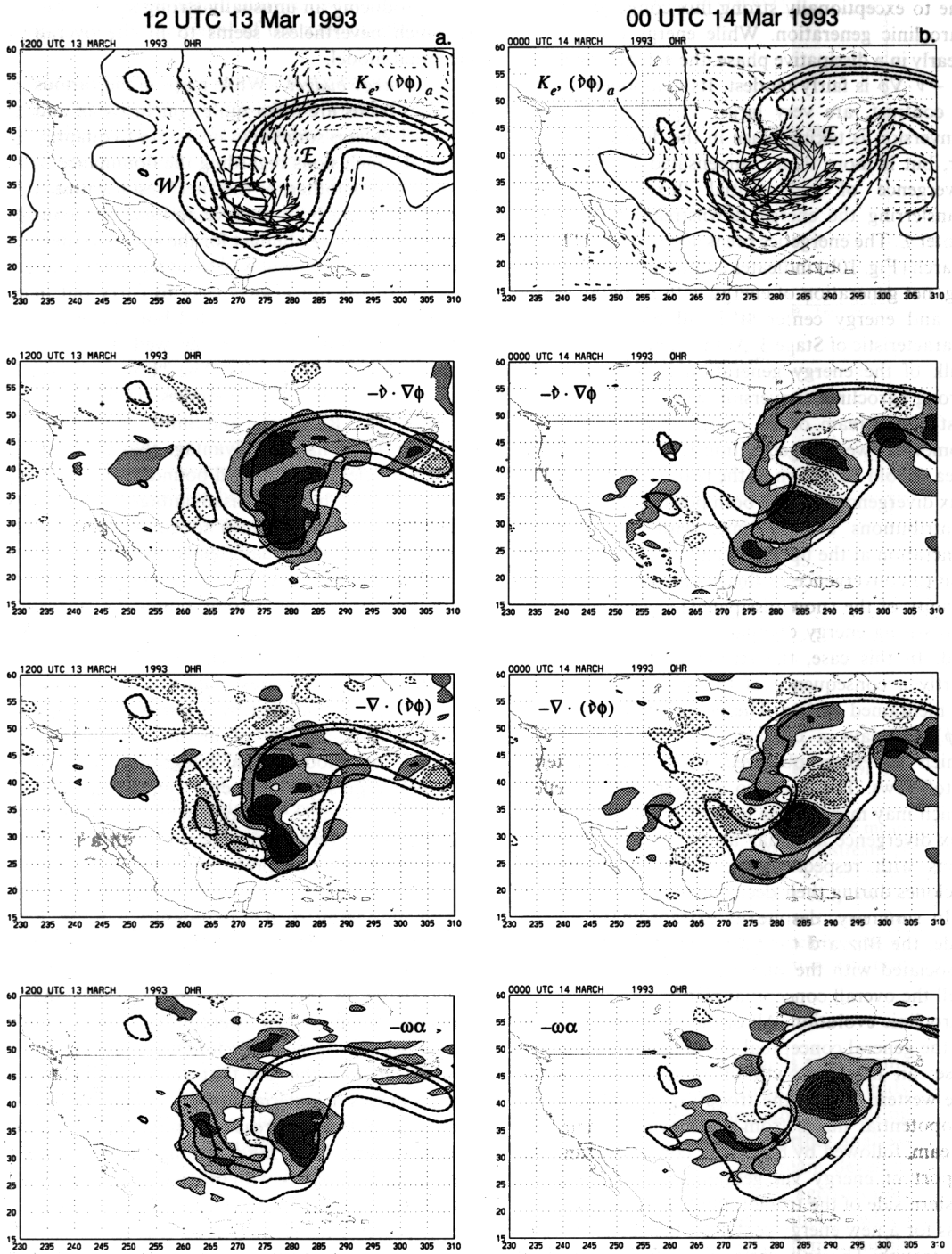

Fig. 10. Same as Fig. 7, but for (a) 1200 UTC 13 March and (b) 0000 UTC 14 March. Vector size has been reduced by a factor of 2 in 10(b).

due to exceptionally strong flux convergence and baroclinic generation. While energy center $\mathcal{W}$ is clearly in a dissipative phase, the actual magnitude of $-v \cdot \nabla\phi$ is fairly modest. Its component terms, in contrast, are very large. Vigorous baroclinic conversion is taking place in the descending cold air, but is more than compensated for by strong divergence of geopotential fluxes which are transferring the energy downstream into energy center $\mathcal{E}$. The energetics breakdown for 00 UTC 14 March (Fig. 10b) indicates continued, but decreasing, net generation of energy within energy center $\mathcal{E}$, and energy center $\mathcal{W}$ is all but gone, both characteristic of Stage 3. At this time, however, the bulk of the energy generation in $\mathcal{E}$ is via very strong baroclinic conversion which is taking place just downstream of the energy center maximum. Somewhat weaker generation is continuing in the area of cold advection to the rear of the storm. The flux divergence displays both positive and negative contributions at this time, with the strongest generation at the upstream end of energy center $\mathcal{E}$ due to convergence of fluxes emanating from the vicinity of the (now dissipated) energy center $\mathcal{W}$, and strong energy dissipation at the downstream end. In this case, the strong divergence is also partly a consequence of the strong $-\omega\alpha$ there, as mentioned earlier. The geopotential flux field, $(v\phi)_a$ displays a characteristic cyclonic pattern which has been observed with several intense cutoff lows. This leads to a "recirculation" effect which may mitigate the losses from the system via flux divergence and may also have some implications with respect to the longevity of intense cyclones during their decay stage.

In summary, despite its extraordinary magnitude, the Blizzard (or more precisely, the trough associated with the Blizzard) appears to fit quite well the overall conceptual picture of downstream baroclinic evolution. All of the important features of the general conceptual picture are found in this case: an initial growth of an energy center on the western side of the trough due to convergent geopotential fluxes from a decaying system upstream, followed by baroclinic conversion and the export of energy via geopotential fluxes to the eastern side of the trough, then an analogous process for a new energy center on the eastern side of the trough. The only variation on this sequence in the case of the Blizzard was the exceptional and prolonged period of energy growth in the eastern center, producing an unusually strong system, but one which nevertheless seems to fit the overall conceptual model.

4.2.1. Energy budget. While maps of the various energetics terms are often quite conclusive in and of themselves, it is sometimes necessary to quantify the visual conclusions regarding the dominance of one term over another, or the "net" result within a region containing both positive and negative contributions. An energy budget for the energy centers would seem to be an ideal way to address this need. However, this is not always easy to carry out in practice, and great care is needed both in setting up the integration procedure as well as in the interpretation of the results. The "box method" used in some diagnostic studies (Chen and Del'Osso, 1987; Robertson and Smith, 1983; Dare and Smith, 1984) has the advantage that it defines an area with clearly delineated boundaries. Unfortunately, it also has the disadvantage that it is difficult to define a box which adequately confines the system, and one usually ends up with a box that either includes fragments systems which are not of interest or has strong boundary fluxes, clouding the interpretation.

A more sophisticated method which would follow the system of interest might be to choose a volume which is bounded by a particular energy contour, and a number of methods have been evaluated for choosing an integration volume which best represents an energy center. The best alternative procedure was one which, while not ideal, produced very useful insights with a minimum of interpretation problems (O&K, O&S). From an examination of the vertical average of the eddy kinetic energy, such as that depicted in Fig. 7, it is generally possible to choose a closed contour bounding a region which can be said to define the energy center of interest. This method has the advantage that it focuses attention on the area of concern and, in large part, follows it during its evolution, despite the fact that such a boundary is by no means a material surface. It has the disadvantage that such areas often fragment into multiple regions, requiring summing of more than one volume, or coalesce with other areas, requiring surgical snipping along carefully chosen lines in order to preserve the identity of an "energy center". It can also be difficult to choose a single K_e value which is appropriate for use throughout the entire growth and decay cycle of the center. A smaller K_e

value which might be necessary when the energy level is low in order to capture the entity of interest could encompass an area larger than the center of interest when the energy levels are much higher, and coalescence of centers becomes problematic. Nevertheless, however arbitrary it might seem, this algorithm has proven very successful in documenting the relative roles of processes within energy centers. And, while no one method is fully satisfactory, this approach at least provides some quantitative measure of the relative importance of baroclinic conversion and flux divergence as a function of time during the evolution of the system.

In the present case, the kinetic energy of centers $\mathcal{W}$ and $\mathcal{E}$ were integrated over the volume bounded in the horizontal by the 100 $m^2 s^{-2}$ and 350 $m^2 s^{-2}$ contour of the vertical average of K_e, respectively, and in the vertical by the 50 mb surface and the earth's surface. The resulting integrals of K_e are shown in the top panel of Fig. 11. Note both the dramatic growth of the integrated energy of the blizzard, as well as its substantially larger magnitude relative to energy center $\mathcal{W}$ (especially in light of the different K_e values used to bound the volumes). Clearly, the growth of energy center $\mathcal{E}$ is not merely result of the transfer of energy from its upstream predecessor. A major source of energy must have been tapped to fuel such growth.

The middle panels of Fig. 11 summarize the primary energy generation terms, which were integrated over the same volumes and then expressed as growth rates by dividing through by the integral of the energy. This approach facilitates the comparison of the phenomena responsible for the development of two centers of greatly different energy levels. One must be careful, however, not to lose sight of the fact that the actual growth of energy is proportional to the actual energy of each of the two centers. The integrals indicate that the $-v \cdot \nabla\phi$ term is almost entirely responsible for the energy generation, with kinetic energy flux divergence and Reynolds stress terms constituting relatively minor contributors. Note, in particular, the burst of growth experienced by energy center $\mathcal{W}$ at 12 UTC 11 March, and by energy center $\mathcal{E}$ at its inception at 00 UTC 13 March. Recall that the 2-dimensional depictions showed, visually, strong geopotential fluxes into the centers at these times.

The role of the geopotential fluxes is quantified in the bottom panels of Fig. 11, which show a further breakdown of energy sources in terms of

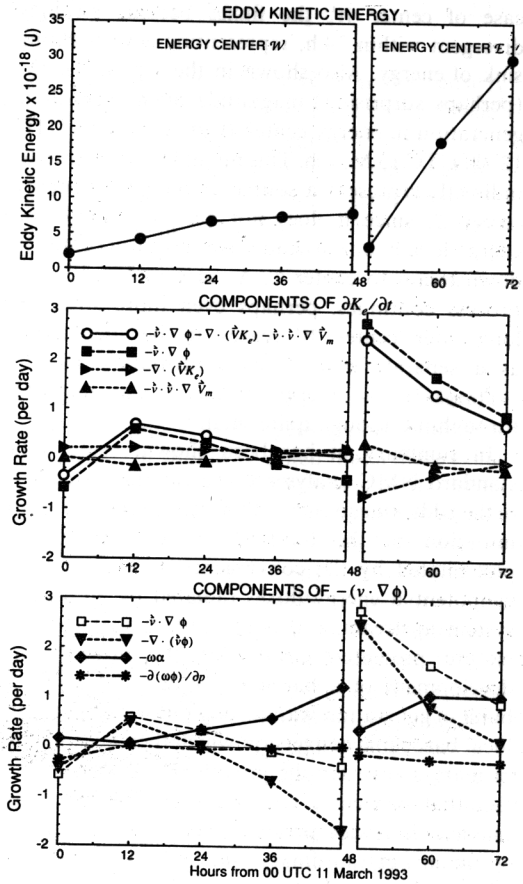

Fig. 11. Volume integrals over energy centers $\mathcal{W}$ (left panels) and $\mathcal{E}$ (right panels), using a bounding K_e contour of 100 and 350 $m^2 s^{-2}$, respectively (see text) for the period 0000 UTC 11 March to 0000 UTC 14 March. Upper panel: eddy kinetic energy. Middle panel: energy generation via $-v\cdot\nabla\phi$, K_e flux convergence ($-\nabla\cdot(VK_e)$, where V is the total wind), Reynolds stress ($-v\cdot v\nabla V_m$), and the sum of all three, yielding a measure of total energy generation. Lower panel: $-v\cdot\nabla\phi$ and its component terms, geopotential flux convergence $-\nabla\cdot(v\phi)$, baroclinic generation $-\omega\alpha$, and pressure work term $-\partial(\omega\phi)/\partial p$.

the components of $-v\cdot\nabla\phi$. These integrals reveal that the bursts of growth early in the development cycle for each center were almost entirely due to geopotential flux convergence. However, in the case of energy center $\mathcal{E}$, flux convergence became secondary within 12 h to baroclinic conversion, $-\omega\alpha$, and was negligible after another 12 h. In the

case of center $\mathcal{W}$, the fluxes became strongly divergent within 24 h, representing a very strong sink of energy. Also shown in these panels is the (perhaps surprising) magnitude of the baroclinic generation in energy center $\mathcal{W}$ at around 12 UTC 12–00 UTC 13 March. This might be considered to indirectly represent a source of energy for energy center $\mathcal{E}$, since it does not act to increase the energy locally but instead fluxes it out of center $\mathcal{W}$ downstream to center $\mathcal{E}$. As seen in Fig. 10, this process continues, perhaps even more strongly, long after center $\mathcal{W}$ ceases to be identifiable as a separate entity. The contribution due to $-\partial(\omega\phi)/\partial p$ for energy center $\mathcal{E}$ was negative throughout, though quite small.

In summary, it has been shown, using only standard NMC analyses and a careful evaluation of the eddy kinetic energy budget, that the explosive initiation of the blizzard of '93 was indeed precipitated by the convergence of ageostrophic geopotential energy fluxes radiated by an energy system upstream, consistent with the conceptual picture presented earlier for the downstream development of a baroclinic system. This initial burst of generation was quickly followed by strong local baroclinic conversion which then became the primary source for the growth of the storm. The fact that baroclinic conversion in this case was massive and widespread draws attention to this storm as a extraordinary and explosive event, but the fact remains that it nevertheless adheres quite closely to what appears to be a robust conceptual explanation for baroclinic development in general, and the growth and transfer of eddy kinetic energy in particular.

5. Summary

Building on the results from idealized and case studies completed to date, a conceptual picture has been advanced which describes, from an energetics standpoint, the entire evolution of a baroclinic system, and which complements the classical theories of cyclone development. Here, the "system" includes not only the cyclone, but the entire trough/ridge pattern with which it is associated. Ageostrophic geopotential fluxes are shown to be key to explaining the growth and dissipation of eddy kinetic energy centers within the system. These fluxes, which are strongest at upper levels, point downstream because of the supergeostrophic nature of the winds through the ridge and subgeostrophic nature in the trough. The convergence/divergence of these fluxes have been shown to represent a critical source/sink of kinetic energy in the downstream development of eddy kinetic energy centers within baroclinic systems. In addition, because these vectors accurately describe the direction of energy dispersion, they can be extremely valuable in quantifying the role of neighboring systems in local development.

The process of "downstream baroclinic evolution", as presented here, is composed of three basic stages. In *Stage 1*, a pre-existing trough with an associated eddy kinetic energy center is assumed to be located upstream of an incipient trough. This older energy center loses energy primarily via ageostrophic geopotential fluxes directed downstream through the ridge. These fluxes are deposited on the western side of the developing trough, increasing the geopotential height gradient and generating a new energy center there. Energy centers such as these are manifestations of what have come to be referred to as "jet streaks".

In *Stage 2*, the new energy center on the west side of the developing trough grows vigorously, partly due to continued convergence of fluxes from the decaying system upstream, but eventually also because of increasing baroclinic generation associated with sinking motion in the cold anomaly. This sinking motion is a consequence of the convergence of the ageostrophic circulation at upper levels, and the baroclinic generation associated with it has proven to be a potent source of energy for a developing system. As the energy center matures, it begins to export energy via geopotential fluxes eastward through the trough, initiating the development of yet another energy center there. While it is the flux convergence at upper levels which initially acts to intensify the new energy center, the circulation it induces eventually enhances the warm ascending motion, implying baroclinic generation which contributes additionally to the kinetic energy. This is precisely the sequence of events characterizing type-B cyclogenesis, as expressed in terms of eddy kinetic energy. The method employed here offers a quantitative tool with which to examine such an event. It is noted that the eddy kinetic energy flux itself, VK_e, has the net effect of translating the energy center primarily toward the east, since most of its meridional transport is compensated for by

removal via geopotential flux divergence to the system downstream. The energy centers thus appear to "jump" from one side of the trough or ridge to the other, similar to the observed behavior of jet streaks, rather than being advected through them. The energy propagates downstream at a group velocity which is greater than the speed of the energy centers themselves (which move with the phase speed).

Lastly, in *Stage 3*, the energy center on the western side of the trough begins to decay as the supply of energy via fluxes from the older upstream system subsides, and also as a consequence of its own export of energy downstream to the center east of the trough. Baroclinic conversion in the western center may continue for some time, but its net effect is to serve primarily as an indirect energy source for the eastern center since most of it is exported via geopotential fluxes. Eventually, strong baroclinic generation in the eastern center becomes its sole source of energy, and how long it continues to grow depends on the intensity of this baroclinic conversion relative to the energy sink represented by flux divergence, barotropic conversion, and friction. Eventually, this center ends up comprising an "upstream system" analogous to the one which initiated the sequence in *Stage 1*.

A new case study was conducted in order to test the limits to which the conceptual picture might apply. Also of interest was whether disturbances could be initiated purely in response to baroclinic generation (type A cyclogenesis). The Blizzard of '93 was chosen as a test case because of its explosive nature, large latent heat release, and development in an apparently quiet environment. Using standard NMC $2.5° \times 2.5°$ gridded analyses, it was shown that the blizzard (or, more precisely, the trough associated with the blizzard) did, in fact, fit the conceptual picture of downstream baroclinic development quite well. While the bulk of the energy generation during the life of the storm was due to baroclinic conversion, geopotential fluxes played a critical role in three respects. First, fluxes from an old, decaying system in the Pacific were convergent over the west coast of North America, creating a kinetic energy center there and modifying the jet to produce a large extension of the overall kinetic energy center well into Mexico. Second, energy fluxes from this extension were strongly convergent over the northwestern coast of the Gulf of Mexico, producing explosive growth of kinetic energy there, followed later by equally explosive baroclinic conversion. Lastly, the kinetic energy generated by the surprisingly vigorous baroclinic conversion in the cold advection on the west side of the trough was very effectively transferred to the energy center on the east side of the trough via the geopotential fluxes. Thus, despite the extraordinary magnitude of the event, even the blizzard of '93 conforms to what appears to be a robust conceptual explanation for baroclinic development in general, and the growth and transfer of eddy kinetic energy in particular.

An understanding of the process of downstream baroclinic evolution may have important implications for the predictability of baroclinic systems. Given the fact that baroclinic evolution can depend strongly on remote forcing via energy fluxes, accurate handling of these fluxes during the data assimilation process should result in improved forecasts. Moreover, under environmental conditions in which downstream development leads to packets of eddies with a life span much longer than individual eddies, the detection of such packets and energy transfer processes may also impact the longer range predictability of such systems.

6. Acknowledgments

The authors wish to express their thanks to Brian Gross, Bob Tuleya, Jerry Mahlman, and Isaac Held for discussions and suggestions that improved and clarified this paper, to Eugenia Kalnay for discussions related to her preliminary analysis of the Blizzard of '93, and to Jeff Varanyak for his assistance in figure preparation.

REFERENCES

Bluestein, H. B. 1993. *Synoptic-dynamic meteorology in midlatitudes*. Oxford University Press, 594 pp.

Chang, K. M. 1993. Downstream development of baroclinic waves as inferred from regression analysis. *J. Atmos. Sci.* **50**, 2038–2053.

Chang, K. M. and Orlanski, I. 1993. On the dynamics of storm tracks. *J. Atmos. Sci.* **50**, 999–1015.

Chang, K. M. and Orlanski, I. 1994. On energy flux and group velocity of waves in baroclinic flows. *J. Atmos. Sci.* **51**, 3823–3828.

Chen, S.-J. and Del'Osso, L. 1987. A numerical case study of East Asian cyclogenesis. *Mon. Wea. Rev.* **115**, 477–487.

Dare, P. M. and Smith, P. J. 1984. A comparison of observed and model energy balance for an extratropical cyclone system. *Mon. Wea. Rev.* **112**, 1289–1308.

Davis, C. A. and Emanuel, K. E. 1991. Potential vorticity diagnostics of cyclogenesis. *Mon. Wea. Rev.* **119**, 1929–1953.

Farrell, B. 1982. The initial growth of disturbances in a baroclinic flow. *J. Atmos. Sci.* **39**, 1663–1686.

Hoskins, B. J. 1990. Theory of extratropical cyclones. Extratropical Cyclones (Chapter 5), Palmen Memorial Volume (C. Newton and E. Holopainen, eds.). American Meteorological Society, Boston, 63–80.

Hoskins, B. J., McIntyre, M. E. and Robertson, A. W. 1985. On the use and significance of isentropic potential vorticity maps. *Quart. J. Roy. Meteor. Soc.* **111**, 877–946.

Hovmöller, E. 1949. The trough and ridge diagram. *Tellus* **1**, 62–66.

Lee, S. and Held, I. M. 1993. Baroclinic wave packets in models and observations. *J. Atmos. Sci.* **50**, 1413–1428.

Lim, G. H. and Wallace, J. M. 1991. Structure and evolution of baroclinic waves as inferred from regression analysis. *J. Atmos. Sci.* **48**, 1718–1732.

Lorenz, E. N. 1955. Available potential energy and the maintenance of the general circulation. *Tellus* **7**, 157–167.

Lott, N. 1993. *The big one! A review of the 12–14 March 1993 "Storm of the century"*. NCDC/NOAA Tech. Rep. 93-01, 25 pp.

Namias, J. and Clapp, P. F. 1944. Studies of the motion and development of long waves in the westerlies. *J. Meteor.* **1**, 57–77.

Newton, C. W. and Palmen, E. 1963. Kinematic and thermal properties of a large amplitude wave in the westerlies. *Tellus* **15**, 99–119.

Orlanski, I. and Chang, K. M. 1993. Ageostrophic geopotential fluxes in downstream and upstream development of baroclinic waves. *J. Atmos. Sci.* **50**, 212–225.

Orlanski, I. and Katzfey, J. J. 1991. The life cycle of a cyclone wave in the Southern Hemisphere: Part I: Eddy energy budget. *J. Atmos. Sci.* **48**, 1972–1998.

Orlanski, I. and Sheldon, J. 1993. A case of downstream baroclinic development over western North America. *Mon. Wea. Rev.* **121**, 2929–2950.

Pedlosky, J. 1987. *Geophysical fluid dynamics*. Springer-Verlag, 710 pp.

Petterssen, S. and Smebye, S. J. 1971. On the development of extratropical cyclones. *Quart. J. R. Met. Soc.* **97**, 457–482.

Peixoto, J. P. and Oort, A. H. 1992. *Physics of climate*. American Institute of Physics, 520 pp.

Randel, W., Stevens, D. and Stanford, J. 1987. A study of planetary waves in the southern winter troposphere and stratosphere. Part II: Life cycle. *J. Atmos. Sci.* **44**, 936–949.

Robertson, F. R. and Smith, P. J. 1983. The impact of model moist processes on the energetics of extratropical cyclones. *Mon. Wea. Rev.* **111**, 723–744.

Sanders, F. and Gykum, J. R. 1980. Synoptic-dynamic climatology of the "bomb". *Mon. Wea. Rev.* **108**, 1589–1606.

Shapiro, M. A. 1982. *Mesoscale weather systems of the central United States*. CIRES/NOAA Tech. Rep., University of Colorado, 78 pp.

Simmons, A. J. and Hoskins, B. J. 1979. The downstream and upstream development of unstable baroclinic waves. *J. Atmos. Sci.* **36**, 1239–1260.

Thorncroft, C. D. and Hoskins, B. J. 1990. Frontal cyclogenesis. *J. Atmos. Sci.* **47**, 2317–2236.

Uccellini, L. W. and Johnson, D. R. 1979. The coupling of upper and lower level jet streaks and implications for the development of severe convective storms. *Mon. Wea. Rev.* **107**, 682–703.